Published for SISSA by Springer

Received: April 3, 2018
Accepted: June 12, 2018
Published: June 20, 2018

Measurement of the inelastic pp cross-section at a centre-of-mass energy of 13 TeV



The LHCb collaboration

E-mail: Michael.Schmelling@mpi-hd.mpg.de

Abstract: The cross-section for inelastic proton-proton collisions at a centre-of-mass energy of 13 TeV is measured with the LHCb detector. The fiducial cross-section for inelastic interactions producing at least one prompt long-lived charged particle with momentum $p > 2\,\text{GeV}/c$ in the pseudorapidity range $2 < \eta < 5$ is determined to be $\sigma_{\text{acc}} = 62.2 \pm 0.2 \pm 2.5\,\text{mb}$. The first uncertainty is the intrinsic systematic uncertainty of the measurement, the second is due to the uncertainty on the integrated luminosity. The statistical uncertainty is negligible. Extrapolation to full phase space yields the total inelastic proton-proton cross-section $\sigma_{\text{inel}} = 75.4 \pm 3.0 \pm 4.5\,\text{mb}$, where the first uncertainty is experimental and the second due to the extrapolation. An updated value of the inelastic cross-section at a centre-of-mass energy of 7 TeV is also reported.

Keywords: Global features, Hadron-Hadron scattering (experiments), Minimum bias

ArXiv ePrint: 1803.10974

Open Access, Copyright CERN,
for the benefit of the LHCb Collaboration.
Article funded by SCOAP^3.

https://doi.org/10.1007/JHEP06(2018)100

JHEP06(2018)100

Contents

1 Introduction 1

2 Detector and data samples 1

3 Analysis method 3

4 Measurement of the fiducial cross-section 5

5 Extrapolation to full phase space 6

6 Summary and conclusions 8

The LHCb collaboration 13

JHEP06(2018)100

1 Introduction

The inelastic cross-section is a fundamental quantity in the phenomenology of high-energy hadronic interactions that are studied at particle accelerators. It is also important for astroparticle physics, *e.g.* in the description of extensive air showers induced by cosmic rays hitting the atmosphere of the Earth [1], or for the modelling of the transport of cosmic ray particles in the interstellar medium [2, 3]. Since quantum chromodynamics cannot yet be solved in the nonperturbative regime, it is currently not possible to calculate the inelastic cross-section from first principles. Models based on Regge phenomenology predict, within the limits of the Froissart-Martin bound [4, 5], an increase with energy according to a power law [6]. Asymptotically the Froissart-Martin bound grows proportional to $(\ln s)^2$, where s is the square of the centre-of-mass energy of the collision. Although originally derived for the total cross-section, this bound has been shown to apply also for the inelastic cross-section [7].

This paper presents a measurement of the inelastic proton-proton cross-section at $\sqrt{s} = 13\,\text{TeV}$, which is the highest collision energy reached so far at any particle accelerator. The measurement is performed with the LHCb detector in the pseudorapidity range $2 < \eta < 5$. Other measurements of the inelastic proton-proton cross-section at LHC energies have been reported by the ALICE [8] (2.76 and 7 TeV), ATLAS [9–12] (7, 8 and 13 TeV), CMS [13, 14] (7 and 13 TeV), LHCb [15] (7 TeV) and TOTEM [16–21] (7, 8 and 13 TeV) collaborations, covering also central and very forward rapidities.

2 Detector and data samples

The LHCb detector [22, 23] is a single-arm forward spectrometer, designed for the study of particles containing b or c quarks. The detector includes a high-precision tracking system

consisting of a silicon-strip vertex detector surrounding the interaction region, a large-area silicon-strip detector located upstream of a dipole magnet with a bending power of about 4 Tm, and three stations of silicon-strip detectors and straw drift tubes placed downstream of the magnet. The tracking system provides a measurement of momentum p of charged particles with a relative uncertainty that varies from 0.5% at low momentum to 1.0% at 200 GeV/c. The minimum distance of a track to a primary vertex (PV), the impact parameter, is measured with a resolution of $(15 + 29/p_{\mathrm{T}})\,\mu$m, where p_{T} is the component of the momentum transverse to the beam, in GeV/c. Different types of charged hadrons are distinguished using information from two ring-imaging Cherenkov detectors. Photons, electrons and hadrons are identified by a calorimeter system consisting of scintillating-pad and preshower detectors, an electromagnetic calorimeter and a hadronic calorimeter. Muons are identified by a system composed of alternating layers of iron and multiwire proportional chambers.

The online event selection for this measurement is based on unbiased triggers, which randomly accept a small subset of all bunch crossings. The bulk of the recorded data are from collisions between leading bunches in the bunch trains of the LHC filling pattern [24], thus largely reducing background from previous bunch crossings. Data were collected for both polarities of the LHCb dipole magnet to test for magnetic-field dependent systematic effects. The total data sample consists of 691 million events in 49 runs from 8 LHC fills, recorded in 2015 between July 8 and August 13. A run corresponds to a data set recorded under stable conditions and for a duration of up to one hour. Data from a long fill are spread over several runs.

The integrated luminosity of this data set was determined in a separate study. The standard way to determine the relative luminosity in LHCb is based on continuous monitoring of the rate of interactions with at least two tracks reconstructed in the vertex detector [25]. This is done online by applying the empty-event counting method (see section 3) to a dedicated set of randomly sampled events that are partially reconstructed in the trigger. The integrated luminosity is obtained by dividing the number of those interactions by their "reference" cross-section. With independent data from a dedicated LHC fill at $\sqrt{s} = 13$ TeV, this reference cross-section was determined to be 63.4 mb with an uncertainty of 3.9%, using the beam-gas imaging method as described in ref. [25]. For the unbiased data from leading bunch crossings the number of partially reconstructed events for the luminosity measurement is much smaller than the number of fully reconstructed events available for offline analysis. Therefore, to obtain precise relative luminosity measurements that permit sensitive studies of systematic effects, the empty-event counting method is applied to the fully reconstructed events. The analysis is performed per leading bunch crossing and in time intervals of $O(1\mathrm{s})$, thereby minimising systematic uncertainties due to differences in the individual bunch currents and variations of the instantaneous interaction rates. Differences between the partial reconstruction in the trigger and the full reconstruction result in a difference of about 1% in the visible interaction rates. The ratio was measured with a statistical uncertainty of 0.2%. Accounting for this difference and taking the absolute calibration from the beam gas imaging method, a total integrated luminosity of 10.7 nb^{-1} is obtained for the full data set, with an uncertainty of 4%, which is domi-

JHEP06(2018)100

nated by the 3.9% uncertainty on the reference cross-section. Additional contributions are the 0.2% statistical uncertainty of the cross-calibration factor and a 0.8% difference when requiring at least one reconstructed primary vertex instead of two vertex-detector tracks.

Simulated events are used to study the detector response and effects of the reconstruction chain. In the simulation, proton-proton collisions for both magnet polarities are generated using Pythia 8 [26, 27] with a specific LHCb configuration [28]. Decays of hadronic particles are described by EvtGen [29], in which final-state radiation is generated using Photos [30]. The interaction of the generated particles with the detector, and its response, are implemented using the Geant4 toolkit [31, 32] as described in ref. [33].

3 Analysis method

The primary measurement is a fiducial cross-section, defined as the cross-section for proton-proton collisions with at least one prompt, long-lived charged particle with momentum $p > 2\,\text{GeV}/c$ and pseudorapidity in the range $2 < \eta < 5$. A particle is defined as "long-lived" if its lifetime is larger than 30 ps, and it is prompt if it is produced directly in the primary collision or if none of its ancestors is long-lived. At the LHCb experiment a lifetime of 30 ps corresponds to a typical flight length of $O(100)$ mm. According to this definition, for instance, ground-state hyperons are long-lived, but not any particle containing charm or beauty quarks.

The experimental selection of prompt long-lived charged particles requires well reconstructed charged tracks with momentum $p > 2\,\text{GeV}/c$ and $2 < \eta < 5$ that traverse the entire LHCb tracking system and have an estimated point of origin located longitudinally (along the beam direction) within 200 mm and transversally within 0.4 mm of the average PV position in the run. From a parametrisation of the PV density by a three-dimensional Gaussian function, the estimated point of origin is determined as that point on the particle trajectory, parametrised by a straight line, where the PV density is highest. With this selection all events can be used in the analysis, independently of whether a PV was reconstructed. The above requirements select almost exclusively inelastic interactions. From about 8.7 million elastic proton-proton scattering processes in the simulation none is accepted.

The cross-section measurement exploits the fact that the recorded event sample is unbiased, with the number of inelastic interactions per event drawn from a Poisson distribution. The average number of interactions μ per event can then be inferred from the fraction p_0 of empty events, $\mu = -\ln p_0$, and for a given number N_{evt} of events the fiducial cross-section is given by

$$\sigma_{\text{acc}} = \frac{(\mu - \mu_{\text{bkg}})N_{\text{evt}}}{\mathcal{L}} \,, \tag{3.1}$$

where $\mathcal{L}$ is the integrated luminosity of the event sample. The number μ_{bkg} of background interactions per event is estimated from bunch crossings where only the bunch from one of the beams was populated. The largest background levels are found for the first LHC fill used in the analysis, with μ_{bkg}/μ around 1%. The cross-section measurement is performed

JHEP06(2018)100

separately for all leading bunch crossings, and in time intervals of $O(8\text{s})$ to follow variations of the interaction rate during a run.

The determination of the empty-event probability p_0 takes into account that, because of inefficiencies, events may be wrongly tagged as empty, and that events which have no prompt long-lived charged particle inside the fiducial region can be classified as non-empty because of misreconstructed tracks. For the measurement presented here, the detector related effects are accounted for by an approach that relates p_0 to the observed charged track multiplicity distribution inside the fiducial region.

A good approximation for the low-multiplicity events that dominate the empty-event counting is the assumption that on average the detector response is the same for every true particle. In other words, the multiplicity distribution of reconstructed tracks is assumed to be the same for every true particle. As shown below, in this case p_0 can be determined from the observed multiplicity distribution of long-lived prompt charged tracks in the detector acceptance.

The relation between p_0 and experimentally accessible information can be derived starting from the probability generating function (PGF) of the observed multiplicity distribution $F_q(x) = \sum_n q_n x^n$, where the probability q_n to observe n tracks is weighted by the n-th power of a continuous variable x. It can be shown that the PGF of a convolution of two discrete probability distributions is the product of the individual PGFs. Introducing $G(x)$ as the PGF of the multiplicity distribution that is reconstructed for a single true particle, the PGF for the case of k true particles is the PGF of the convolution of k single particle distributions, *i.e.* the k-th power $G^k(x)$. Weighting each true multiplicity k with its probability p_k, the relation between the PGF of the observed multiplicity distribution q_n and the true multiplicity distribution p_k is given by

$$F_q(x) = \sum_{n=0}^{\infty} q_n x^n = \sum_{k=0}^{\infty} p_k \, G^k(x) \; . \tag{3.2}$$

The true empty-event probability p_0 can be inferred by setting $x = \alpha$ such that $G(\alpha) = 0$, which yields

$$p_0 = \sum_{n=0}^{\infty} q_n \alpha^n \; . \tag{3.3}$$

The parameter α is the only detector-related parameter of the analysis. It is an unfolding parameter that relates p_0 to the observed charged particle multiplicity distribution in the fiducial region. For an ideal detector it would be zero. For a given experiment the value of α depends mainly on the average reconstruction efficiency. Assuming for example a binomial detector response, where a particle is either reconstructed with efficiency ε or missed, one has $G(x) = (1 - \varepsilon) + \varepsilon x$ and thus $\alpha = (\varepsilon - 1)/\varepsilon$, which is always negative. When taking p_0 and q_n from fully simulated events and solving eq. (3.3) for α, one obtains an effective parameter that also accounts for higher-order effects due to background tracks and nonlinear detector response.

For proton-proton collisions at high centre-of-mass energies, where inelastic interactions have high multiplicity final states, and for data with a small average number of

JHEP06(2018)100

simultaneous interactions per bunch crossing, the cross-section measurement has only very little sensitivity to the exact value of α. The measurements presented below are based on events with μ in the range between 0.4 and 1.4 and values of q_0 that are at least an order of magnitude larger than the values q_n for $n > 0$. With a typical value $\alpha \approx -0.6$ the values of p_0 are on average only about 3% smaller than their leading-order estimates q_0, which results in robust cross-section measurements even in case of sizeable systematic uncertainties on α.

4 Measurement of the fiducial cross-section

The inelastic fiducial cross-section is determined separately for all runs recorded with unbiased triggers and, within a run, all leading bunch crossings. In total 243 independent measurements are done, with different filling patterns of the LHC, different bunch currents and both magnet polarities. For each measurement an initial estimate for the unfolding parameter α is obtained from a simulation that has been weighted to match the average reconstructed track multiplicity in data. This initial value is then corrected to account for differences between data and simulation in the average track reconstruction efficiency and the average fraction of misreconstructed tracks. The efficiency correction uses an independent calibration for the analysed data set, determined as described in ref. [34]. The fraction of misreconstructed tracks is estimated from the fraction of tracks rejected by the track selection criteria, with a constant of proportionality taken from simulation. The observed differences between data and simulation are propagated into α by means of a simplified model that relates it to the average track reconstruction efficiency and the fraction of misreconstructed tracks.

The individual cross-section measurements are combined in a weighted average, assuming uncorrelated statistical and fully correlated systematic uncertainties. The weight of each measurement is proportional to the integrated luminosity of the corresponding data set, resulting in an overall fiducial cross-section $\sigma_{\text{acc}} = 62.237 \pm 0.002\,\text{mb}$, where the uncertainty is purely statistical. The contributions to the systematic uncertainty are summarised in table 1. The dominant contribution is the 4% uncertainty on the integrated luminosity. The intrinsic uncertainty of the analysis is driven by a 16% uncertainty on the unfolding parameter α, which propagates into a 0.25% systematic uncertainty on σ_{acc}. The largest contribution is due to the difference between either determining α from all simulated events or only from events with particles inside the fiducial region. The systematic uncertainties due to the efficiency calibration and the differences in the fraction of misreconstructed tracks between data and simulation, where the full size of the correction is assigned as a systematic uncertainty, are slightly smaller.

Figure 1 shows a comparison of the overall fiducial cross-section with the averages within the individual LHC fills. While within a fill all measurements are found to be consistent within their statistical uncertainties, small but significant differences are seen between fills. These differences are found to be correlated with quantities not studied in the simulation, namely the vertical position and extension of the luminous region and, to a lesser extent, the background level seen in the data. The spread associated to those

JHEP06(2018)100

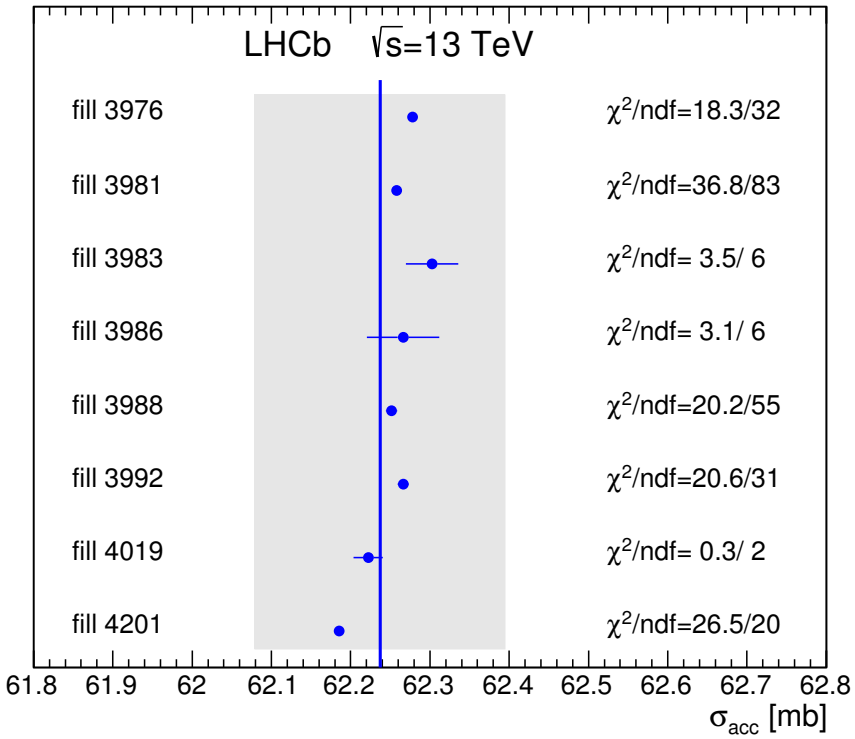


Figure 1. Overall fiducial cross-section (vertical line), compared to the averages of the individual results in different LHC fills. The error bars indicate the statistical uncertainties. The grey band indicates the systematic uncertainty on the overall average due to the unfolding parameter α. The χ^2-values for the averages inside a fill are calculated with only the statistical uncertainties and the number of degrees of freedom (ndf) is one less than the number of individual results contributing to the average. Systematic uncertainties inferred from the observed spread between the fills are discussed in the text.

variables corresponds to an additional systematic uncertainty of 0.05%. Also given in figure 1 are the χ^2-values of the individual averages, calculated with only the statistical uncertainties. Inspection of the χ^2-values shows that, except for the last fill, the agreement between the results within one fill is actually better than expected. This is due to the fact that the luminosity calibration and the inelastic cross-section measurement are correlated by the use of information recorded by the vertex detector. The average for the last fill, which in comparison to the others has an enlarged χ^2 value, is dominated by two runs with more than 100 million events. This points to the existence of additional systematic effects of about the size of the statistical uncertainty of this average, which in view of the other uncertainties are negligible. Cross-checks from variations of the track selection criteria show no indication of additional systematic effects.

5 Extrapolation to full phase space

The extrapolation from the fiducial cross-section $\sigma_{\rm acc}$ to the total inelastic cross-section $\sigma_{\rm inel} = F_{\rm T}\,\sigma_{\rm acc}$ follows the same approach as in ref. [15]. The extrapolation factor $F_{\rm T}$

JHEP06(2018)100

Source	Relative uncertainty
Integrated luminosity	4.00%
Unfolding parameter α	0.25%
— Interactions not in acceptance	0.18%
— Efficiency	0.15%
— Misreconstructed tracks	0.12%
Luminous region and background	0.05%
Total	4.01%

Table 1. Summary of systematic uncertainties on the fiducial cross-section. For the contribution from the unfolding parameter α a breakdown into the individual components is given.

	f_X		v_X		$n_{\mathrm{ch},X}$	
	mean	s.d.	mean	s.d.	mean	s.d.
Non-diffractive (ND)	0.720	0.012	0.9963	0.0005	17.94	1.45
Single diffractive (SDA)	0.083	0.003	0.7154	0.0051	8.11	0.52
Single diffractive (SDB)	0.083	0.003	0.3411	0.0077	7.83	0.44
Double diffractive (DD)	0.114	0.006	0.6263	0.0049	6.15	0.31

Table 2. Properties of Pythia 8.230 proton-proton tunes. Mean values and standard deviations are given for the fractions f_X of the inelastic cross-section, the fractions v_X of interactions inside the acceptance and, for those interactions, the average numbers of long-lived prompt charged particles $n_{\mathrm{ch},X}$ inside the acceptance.

is determined from generator-level simulations. Neglecting interference effects between different contributions, it is assumed that the total inelastic cross-section can be written as an incoherent sum of distinct contributions

$$\sigma_{\mathrm{inel}} = \sum_X \sigma_X \quad \text{with} \quad X \in \{\mathrm{ND}, \mathrm{SDA}, \mathrm{SDB}, \mathrm{DD}\} \; . \tag{5.1}$$

Here σ_{ND} is the non-diffractive cross-section, σ_{SDA} and σ_{SDB} are the single diffractive contributions with the diffractively excited system travelling towards (A) or away (B) from the detector, which have the same cross-section but different contributions to the visible cross-section, and σ_{DD} is the double diffractive cross-section. State-of-the-art event generators are assumed to provide a realistic parametrisation of the properties of the various contributions. This has been studied with the 32 proton-proton tunes that come with Pythia 8.230 [35] and which do not require external libraries. Table 2 gives mean values and standard deviations of the fractions f_X of the inelastic cross-section, the fractions v_X of interactions with at least one prompt long-lived charged particle within the acceptance and, for those interactions, the average multiplicities $n_{\mathrm{ch},X}$ of those particles inside the acceptance.

Given the fractions f_X of the total inelastic cross-section and the fractions of visible interactions v_X, the extrapolation factor F_{T} is

$$F_{\mathrm{T}} = \frac{\sum_X \sigma_X}{\sum_X \sigma_X \, v_X} = \frac{1}{\sum_X f_X \, v_X} \; . \tag{5.2}$$

JHEP06(2018)100

Taking the standard deviations from table 2 as model uncertainties would likely underestimate the uncertainty of the extrapolation factor, since in particular the cross-section fractions have a much smaller spread than the uncertainties obtained in a measurement of the diffractive contributions to the inelastic cross-section, $f_{\mathrm{SD}} = 0.20^{+0.04}_{-0.07}$ and $f_{\mathrm{DD}} = 0.12^{+0.05}_{-0.04}$, performed by the ALICE collaboration at $\sqrt{s} = 7\,\mathrm{TeV}$ [8].

To reduce the model dependence in the determination of F_{T}, the cross-section fractions are considered to be a priori unknown and only subject to the constraint $\sum_X f_X = 1$. The extrapolation factor is estimated from sets $\{f_X\}$ that uniformly sample the subspace defined by this constraint. For each set $\{f_X\}$ the extrapolation factor F_{T} and the average multiplicity $n_{\mathrm{ch}} = \sum_X f_X\, n_{\mathrm{ch},X}$ inside the fiducial region are calculated using v_X and $n_{\mathrm{ch},X}$ from table 2. The spread of the different tunes is propagated into the extrapolation factor by drawing v_X and $n_{\mathrm{ch},X}$ from Gaussian distributions with mean values and standard deviations as given in the table. An additional experimental constraint is imposed by assigning a Gaussian weight $w = \exp(-(n_{\mathrm{ch}} - N)^2/2\sigma_N^2)$ to $\{f_X\}$ and F_{T}, where $N = 13.9 \pm 0.9$ is the average multiplicity per interaction of prompt long-lived charged particles inside the acceptance in the data. The numerical value for this constraint is obtained from the full simulation, tuned to reproduce the observed average multiplicity per event and corrected for differences between data and simulation in the average track reconstruction efficiency and the fraction of tracks that are associated to a true particle.

Figure 2 shows the posterior densities $\rho(f_X)$ and $\rho(F_{\mathrm{T}})$ of the cross-section fractions f_X and the cross-section extrapolation factor F_{T}. The mean values of the fractions of f_X are found to be $f_{\mathrm{SD}}^{\mathrm{sim}} = 0.21$ and $f_{\mathrm{DD}}^{\mathrm{sim}} = 0.18$, consistent with measurements at $\sqrt{s} = 7\,\mathrm{TeV}$ [8]. The resulting cross-section extrapolation factor is $F_{\mathrm{T}} = 1.211 \pm 0.072$, which yields a total inelastic cross-section of

$$\sigma_{\mathrm{inel}} = 75.4 \pm 3.0(\mathrm{exp}) \pm 4.5(\mathrm{extr})\,\mathrm{mb}\ ,$$

where the first uncertainty is due to the experimental uncertainty of the fiducial cross-section and the second due to the cross-section extrapolation. Summing all uncertainties in quadrature one finds $\sigma_{\mathrm{inel}} = 75.4 \pm 5.4\,\mathrm{mb}$.

6 Summary and conclusions

A measurement is presented of the inelastic proton-proton cross-section with at least one prompt long-lived charged particle with momentum $p > 2\,\mathrm{GeV}/c$ in the pseudorapidity range $2 < \eta < 5$. A particle is defined as "long-lived" if its lifetime is larger than 30 ps, and it is prompt if it is produced directly in the primary interaction or if none of its ancestors is long-lived. The measurement is done with the empty-event counting method applied to unbiased data. A total of 691 million events is analysed. The statistical uncertainty of the overall result is negligible. The systematic uncertainty has contributions from the integrated luminosity (4%), the unfolding parameter (0.25%) and vertical location and extension of the luminous region and background levels (0.05%). Adding all uncertainties not related to the integrated luminosity in quadrature, the final result for the fiducial

JHEP06(2018)100

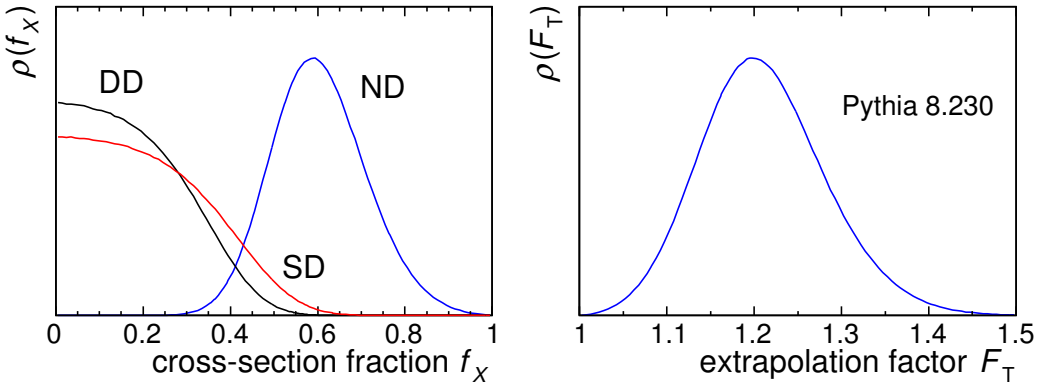


Figure 2. Posterior densities of (left) the cross-section fractions f_X for non-diffractive (ND) double-diffractive (DD) and single-diffractive (SD=SDA+SDB) contributions, and (right) of the extrapolation factor $F_{\rm T}$.

cross-section is

$$\sigma_{\rm acc}(\sqrt{s} = 13\,{\rm TeV}) = 62.2 \pm 0.2 \pm 2.5({\rm lumi})\,{\rm mb}\ .$$

Extrapolating to the full phase space yields a total inelastic cross-section of

$$\sigma_{\rm inel}(\sqrt{s} = 13\,{\rm TeV}) = 75.4 \pm 3.0({\rm exp}) \pm 4.5({\rm extr})\,{\rm mb}\ .$$

Since the publication of a measurement of the inelastic proton-proton cross-section at a centre-of-mass energy of 7 TeV by the LHCb collaboration [15] an improved calibration of the luminosity scale has become available [25]. The new value of the reference cross-section for the integrated luminosity of the data analysed for the previous measurement is 2.7% larger than the initial estimate and the uncertainty has been reduced from 3.5% to 1.7%. With the analysis of ref. [15] unchanged, the updated cross-section is

$$\sigma_{\rm inel}(\sqrt{s} = 7\,{\rm TeV}) = 68.7 \pm 2.1({\rm exp}) \pm 4.5({\rm extr})\,{\rm mb}\ ,$$

which supersedes the previous result. The experimental uncertainty is reduced from 4.3% to 3.0% and the central value shifted up by 2.7%.

A comparison of the total inelastic cross-section measurements from proton-proton collisions at the LHC is shown in figure 3. The new LHCb measurement at $\sqrt{s} = 13\,{\rm TeV}$ is in good agreement with the measurements by the ATLAS [12] and TOTEM [21] collaborations. In the LHC energy range the dependence of the inelastic cross-section on $\sqrt{s}$ is well described by a power law.

Acknowledgments

We express our gratitude to our colleagues in the CERN accelerator departments for the excellent performance of the LHC. We thank the technical and administrative staff at the LHCb institutes. We acknowledge support from CERN and from the national agencies: CAPES, CNPq, FAPERJ and FINEP (Brazil); MOST and NSFC (China); CNRS/IN2P3 (France); BMBF, DFG and MPG (Germany); INFN (Italy); NWO (The

JHEP06(2018)100

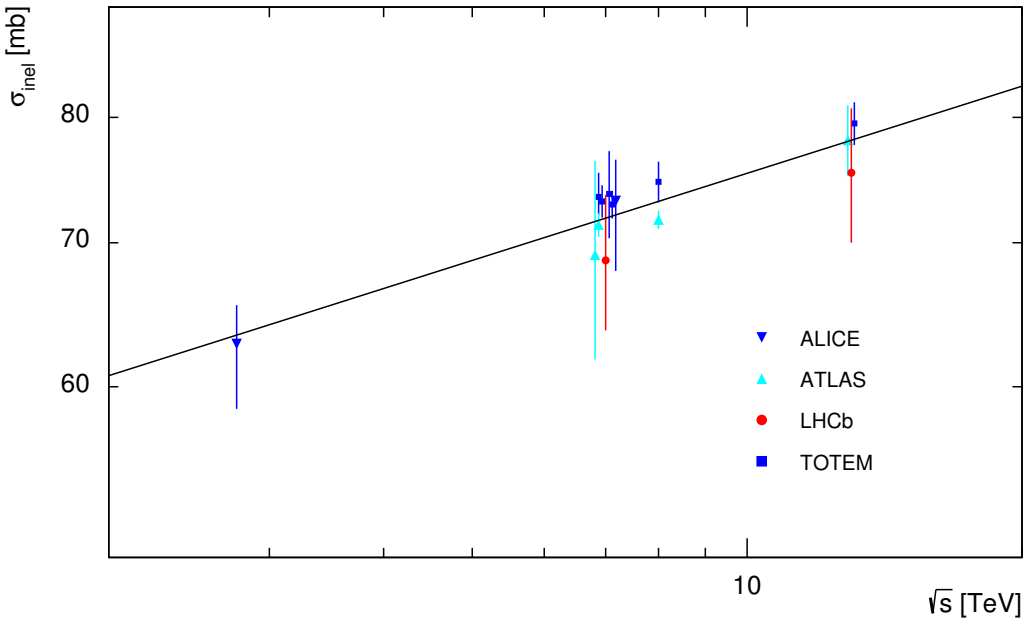


Figure 3. Measurement of the total inelastic proton-proton cross-section at the LHC at centre-of-mass energies of 2.76, 7, 8 and 13 TeV. Results are shown from the ALICE [8], ATLAS [9–12] and TOTEM [16–21] collaborations. For better visibility, measurements at the same energy are drawn at slightly displaced locations. The error bars show the total uncertainties, with positive and negative uncertainties of the respective results independently added in quadrature. The line shows the result from a power-law fit.

Netherlands); MNiSW and NCN (Poland); MEN/IFA (Romania); MinES and FASO (Russia); MinECo (Spain); SNSF and SER (Switzerland); NASU (Ukraine); STFC (United Kingdom); NSF (U.S.A.). We acknowledge the computing resources that are provided by CERN, IN2P3 (France), KIT and DESY (Germany), INFN (Italy), SURF (The Netherlands), PIC (Spain), GridPP (United Kingdom), RRCKI and Yandex LLC (Russia), CSCS (Switzerland), IFIN-HH (Romania), CBPF (Brazil), PL-GRID (Poland) and OSC (U.S.A.). We are indebted to the communities behind the multiple open-source software packages on which we depend. Individual groups or members have received support from AvH Foundation (Germany), EPLANET, Marie Skłodowska-Curie Actions and ERC (European Union), ANR, Labex P2IO and OCEVU, and Région Auvergne-Rhône-Alpes (France), Key Research Program of Frontier Sciences of CAS, CAS PIFI, and the Thousand Talents Program (China), RFBR, RSF and Yandex LLC (Russia), GVA, XuntaGal and GENCAT (Spain), Herchel Smith Fund, the Royal Society, the English-Speaking Union and the Leverhulme Trust (United Kingdom).

Open Access. This article is distributed under the terms of the Creative Commons Attribution License (CC-BY 4.0), which permits any use, distribution and reproduction in any medium, provided the original author(s) and source are credited.

JHEP06(2018)100

References

[1] T. Pierog et al., *EPOS LHC: test of collective hadronization with data measured at the CERN Large Hadron Collider*, *Phys. Rev.* **C 92** (2015) 034906 [arXiv:1306.0121] [INSPIRE].

[2] M. di Mauro, F. Donato, A. Goudelis and P.D. Serpico, *New evaluation of the antiproton production cross section for cosmic ray studies*, *Phys. Rev.* **D 90** (2014) 085017 [arXiv:1408.0288] [INSPIRE].

[3] G. Giesen et al., *AMS-02 antiprotons, at last! Secondary astrophysical component and immediate implications for Dark Matter*, *JCAP* **09** (2015) 023 [arXiv:1504.04276] [INSPIRE].

[4] M. Froissart, *Asymptotic behavior and subtractions in the Mandelstam representation*, *Phys. Rev.* **123** (1961) 1053 [INSPIRE].

[5] A. Martin, *Extension of the axiomatic analyticity domain of scattering amplitudes by unitarity. 1.*, *Nuovo Cim.* **A 42** (1965) 930 [INSPIRE].

[6] A. Donnachie and P.V. Landshoff, *pp and $\bar{p}p$ total cross sections and elastic scattering*, *Phys. Lett.* **B 727** (2013) 500 [*Erratum ibid.* **B 750** (2015) 669] [arXiv:1309.1292] [INSPIRE].

[7] A. Martin, *The Froissart bound for inelastic cross-sections*, *Phys. Rev.* **D 80** (2009) 065013 [arXiv:0904.3724] [INSPIRE].

[8] ALICE collaboration, *Measurement of inelastic, single- and double-diffraction cross sections in proton-proton collisions at the LHC with ALICE*, *Eur. Phys. J.* **C 73** (2013) 2456 [arXiv:1208.4968] [INSPIRE].

[9] ATLAS collaboration, *Measurement of the inelastic proton-proton cross-section at $\sqrt{s} = 7$ TeV with the ATLAS detector*, *Nature Commun.* **2** (2011) 463 [arXiv:1104.0326] [INSPIRE].

[10] ATLAS collaboration, *Measurement of the total cross section from elastic scattering in pp collisions at $\sqrt{s} = 7$ TeV with the ATLAS detector*, *Nucl. Phys.* **B 889** (2014) 486 [arXiv:1408.5778] [INSPIRE].

[11] ATLAS collaboration, *Measurement of the total cross section from elastic scattering in pp collisions at $\sqrt{s} = 8$ TeV with the ATLAS detector*, *Phys. Lett.* **B 761** (2016) 158 [arXiv:1607.06605] [INSPIRE].

[12] ATLAS collaboration, *Measurement of the inelastic proton-proton cross section at $\sqrt{s} = 13$ TeV with the ATLAS detector at the LHC*, *Phys. Rev. Lett.* **117** (2016) 182002 [arXiv:1606.02625] [INSPIRE].

[13] CMS collaboration, *Measurement of the inelastic proton-proton cross section at $\sqrt{s} = 7$ TeV*, *Phys. Lett.* **B 722** (2013) 5 [arXiv:1210.6718] [INSPIRE].

[14] CMS collaboration, *Measurement of the inelastic proton-proton cross section at $\sqrt{s} = 13$ TeV*, arXiv:1802.02613 [INSPIRE].

[15] LHCb collaboration, *Measurement of the inelastic pp cross-section at a centre-of-mass energy of $\sqrt{s} = 7$ TeV*, *JHEP* **02** (2015) 129 [arXiv:1412.2500] [INSPIRE].

[16] G. Antchev et al., *First measurement of the total proton-proton cross section at the LHC energy of $\sqrt{s} = 7$ TeV*, *EPL* **96** (2011) 21002 [arXiv:1110.1395] [INSPIRE].

[17] TOTEM collaboration, G. Antchev et al., *Measurement of proton-proton elastic scattering and total cross-section at $\sqrt{s} = 7$ TeV*, *Europhys. Lett.* **101** (2013) 21002 [INSPIRE].

JHEP06(2018)100

[18] TOTEM collaboration, G. Antchev et al., *Measurement of proton-proton inelastic scattering cross-section at $\sqrt{s} = 7$ TeV*, *Europhys. Lett.* **101** (2013) 21003 [INSPIRE].

[19] TOTEM collaboration, G. Antchev et al., *Luminosity-independent measurements of total, elastic and inelastic cross-sections at $\sqrt{s} = 7$ TeV*, *Europhys. Lett.* **101** (2013) 21004 [INSPIRE].

[20] TOTEM collaboration, G. Antchev et al., *Luminosity-independent measurement of the proton-proton total cross section at $\sqrt{s} = 8$ TeV*, *Phys. Rev. Lett.* **111** (2013) 012001 [INSPIRE].

[21] TOTEM collaboration, G. Antchev et al., *First measurement of elastic, inelastic and total cross-section at $\sqrt{s} = 13$ TeV by TOTEM and overview of cross-section data at LHC energies*, arXiv:1712.06153 [INSPIRE].

[22] LHCb collaboration, *The LHCb detector at the LHC*, 2008 *JINST* **3** S08005 [INSPIRE].

[23] LHCb collaboration, *LHCb detector performance*, *Int. J. Mod. Phys.* **A 30** (2015) 1530022 [arXiv:1412.6352] [INSPIRE].

[24] L. Evans and P. Bryant, *LHC machine*, 2008 *JINST* **3** S08001 [INSPIRE].

[25] LHCb collaboration, *Precision luminosity measurements at LHCb*, 2014 *JINST* **9** P12005 [arXiv:1410.0149] [INSPIRE].

[26] T. Sjöstrand, S. Mrenna and P.Z. Skands, *A brief introduction to PYTHIA 8.1*, *Comput. Phys. Commun.* **178** (2008) 852 [arXiv:0710.3820] [INSPIRE].

[27] T. Sjöstrand, S. Mrenna and P.Z. Skands, *PYTHIA 6.4 physics and manual*, *JHEP* **05** (2006) 026 [hep-ph/0603175] [INSPIRE].

[28] LHCb collaboration, *Handling of the generation of primary events in Gauss, the LHCb simulation framework*, *J. Phys. Conf. Ser.* **331** (2011) 032047 [INSPIRE].

[29] D.J. Lange, *The EvtGen particle decay simulation package*, *Nucl. Instrum. Meth.* **A 462** (2001) 152 [INSPIRE].

[30] P. Golonka and Z. Was, *PHOTOS Monte Carlo: a precision tool for QED corrections in Z and W decays*, *Eur. Phys. J.* **C 45** (2006) 97 [hep-ph/0506026] [INSPIRE].

[31] GEANT4 collaboration, J. Allison et al., *GEANT4 developments and applications*, *IEEE Trans. Nucl. Sci.* **53** (2006) 270 [INSPIRE].

[32] GEANT4 collaboration, S. Agostinelli et al., *GEANT4 — a simulation toolkit*, *Nucl. Instrum. Meth.* **A 506** (2003) 250 [INSPIRE].

[33] LHCb collaboration, *The LHCb simulation application, Gauss: Design, evolution and experience*, *J. Phys. Conf. Ser.* **331** (2011) 032023 [INSPIRE].

[34] LHCb collaboration, *Measurement of the track reconstruction efficiency at LHCb*, 2015 *JINST* **10** P02007 [arXiv:1408.1251] [INSPIRE].

[35] T. Sjöstrand et al., *An introduction to PYTHIA 8.2*, *Comput. Phys. Commun.* **191** (2015) 159 [arXiv:1410.3012] [INSPIRE].

JHEP06(2018)100

The LHCb collaboration

R. Aaij[43], B. Adeva[39], M. Adinolfi[48], Z. Ajaltouni[5], S. Akar[59], J. Albrecht[10], F. Alessio[40], M. Alexander[53], A. Alfonso Albero[38], S. Ali[43], G. Alkhazov[31], P. Alvarez Cartelle[55], A.A. Alves Jr[59], S. Amato[2], S. Amerio[23], Y. Amhis[7], L. An[3], L. Anderlini[18], G. Andreassi[41], M. Andreotti[17,g], J.E. Andrews[60], R.B. Appleby[56], F. Archilli[43], P. d'Argent[12], J. Arnau Romeu[6], A. Artamonov[37], M. Artuso[61], E. Aslanides[6], M. Atzeni[42], G. Auriemma[26], S. Bachmann[12], J.J. Back[50], C. Baesso[62], S. Baker[55], V. Balagura[7,b], W. Baldini[17], A. Baranov[35], R.J. Barlow[56], S. Barsuk[7], W. Barter[56], F. Baryshnikov[32], V. Batozskaya[29], V. Battista[41], A. Bay[41], J. Beddow[53], F. Bedeschi[24], I. Bediaga[1], A. Beiter[61], L.J. Bel[43], N. Beliy[63], V. Bellee[41], N. Belloli[21,i], K. Belous[37], I. Belyaev[32,40], E. Ben-Haim[8], G. Bencivenni[19], S. Benson[43], S. Beranek[9], A. Berezhnoy[33], R. Bernet[42], D. Berninghoff[12], E. Bertholet[8], A. Bertolin[23], C. Betancourt[42], F. Betti[15,40], M.O. Bettler[49], M. van Beuzekom[43], Ia. Bezshyiko[42], S. Bifani[47], P. Billoir[8], A. Birnkraut[10], A. Bizzeti[18,u], M. Bjørn[57], T. Blake[50], F. Blanc[41], S. Blusk[61], V. Bocci[26], T. Boettcher[58], A. Bondar[36,w], N. Bondar[31], S. Borghi[56,40], M. Borisyak[35], M. Borsato[39], F. Bossu[7], M. Boubdir[9], T.J.V. Bowcock[54], E. Bowen[42], C. Bozzi[17,40], S. Braun[12], M. Brodski[40], J. Brodzicka[27], D. Brundu[16], E. Buchanan[48], C. Burr[56], A. Bursche[16], J. Buytaert[40], W. Byczynski[40], S. Cadeddu[16], H. Cai[64], R. Calabrese[17,g], R. Calladine[47], M. Calvi[21,i], M. Calvo Gomez[38,m], A. Camboni[38,m], P. Campana[19], D.H. Campora Perez[40], L. Capriotti[56], A. Carbone[15,e], G. Carboni[25], R. Cardinale[20,h], A. Cardini[16], P. Carniti[21,i], L. Carson[52], K. Carvalho Akiba[2], G. Casse[54], L. Cassina[21], M. Cattaneo[40], G. Cavallero[20,h], R. Cenci[24,t], D. Chamont[7], M.G. Chapman[48], M. Charles[8], Ph. Charpentier[40], G. Chatzikonstantinidis[47], M. Chefdeville[4], S. Chen[16], S.-G. Chitic[40], V. Chobanova[39], M. Chrzaszcz[40], A. Chubykin[31], P. Ciambrone[19], X. Cid Vidal[39], G. Ciezarek[40], P.E.L. Clarke[52], M. Clemencic[40], H.V. Cliff[49], J. Closier[40], V. Coco[40], J. Cogan[6], E. Cogneras[5], V. Cogoni[16,f], L. Cojocariu[30], P. Collins[40], T. Colombo[40], A. Comerma-Montells[12], A. Contu[16], G. Coombs[40], S. Coquereau[38], G. Corti[40], M. Corvo[17,g], C.M. Costa Sobral[50], B. Couturier[40], G.A. Cowan[52], D.C. Craik[58], A. Crocombe[50], M. Cruz Torres[1], R. Currie[52], C. D'Ambrosio[40], F. Da Cunha Marinho[2], C.L. Da Silva[73], E. Dall'Occo[43], J. Dalseno[48], A. Davis[3], O. De Aguiar Francisco[40], K. De Bruyn[40], S. De Capua[56], M. De Cian[12], J.M. De Miranda[1], L. De Paula[2], M. De Serio[14,d], P. De Simone[19], C.T. Dean[53], D. Decamp[4], L. Del Buono[8], B. Delaney[49], H.-P. Dembinski[11], M. Demmer[10], A. Dendek[28], D. Derkach[35], O. Deschamps[5], F. Dettori[54], B. Dey[65], A. Di Canto[40], P. Di Nezza[19], S. Didenko[69], H. Dijkstra[40], F. Dordei[40], M. Dorigo[40], A. Dosil Suárez[39], L. Douglas[53], A. Dovbnya[45], K. Dreimanis[54], L. Dufour[43], G. Dujany[8], P. Durante[40], J.M. Durham[73], D. Dutta[56], R. Dzhelyadin[37], M. Dziewiecki[12], A. Dziurda[40], A. Dzyuba[31], S. Easo[51], U. Egede[55], V. Egorychev[32], S. Eidelman[36,w], S. Eisenhardt[52], U. Eitschberger[10], R. Ekelhof[10], L. Eklund[53], S. Ely[61], A. Ene[30], S. Escher[9], S. Esen[12], H.M. Evans[49], T. Evans[57], A. Falabella[15], N. Farley[47], S. Farry[54], D. Fazzini[21,40,i], L. Federici[25], G. Fernandez[38], P. Fernandez Declara[40], A. Fernandez Prieto[39], F. Ferrari[15], L. Ferreira Lopes[41], F. Ferreira Rodrigues[2], M. Ferro-Luzzi[40], S. Filippov[34], R.A. Fini[14], M. Fiorini[17,g], M. Firlej[28], C. Fitzpatrick[41], T. Fiutowski[28], F. Fleuret[7,b], M. Fontana[16,40], F. Fontanelli[20,h], R. Forty[40], V. Franco Lima[54], M. Frank[40], C. Frei[40], J. Fu[22,q], W. Funk[40], C. Färber[40], E. Gabriel[52], A. Gallas Torreira[39], D. Galli[15,e], S. Gallorini[23], S. Gambetta[52], M. Gandelman[2], P. Gandini[22], Y. Gao[3], L.M. Garcia Martin[71], J. García Pardiñas[39], J. Garra Tico[49], L. Garrido[38], D. Gascon[38], C. Gaspar[40], L. Gavardi[10], G. Gazzoni[5], D. Gerick[12], E. Gersabeck[56], M. Gersabeck[56], T. Gershon[50], Ph. Ghez[4], S. Gianì[41], V. Gibson[49], O.G. Girard[41], L. Giubega[30], K. Gizdov[52], V.V. Gligorov[8], D. Golubkov[32], A. Golutvin[55,69], A. Gomes[1,a], I.V. Gorelov[33], C. Gotti[21,i], E. Govorkova[43], J.P. Grabowski[12], R. Graciani Diaz[38],

JHEP06(2018)100

L.A. Granado Cardoso[40], E. Graugés[38], E. Graverini[42], G. Graziani[18], A. Grecu[30], R. Greim[43], P. Griffith[16], L. Grillo[56], L. Gruber[40], B.R. Gruberg Cazon[57], O. Grünberg[67], E. Gushchin[34], Yu. Guz[37], T. Gys[40], C. Göbel[62], T. Hadavizadeh[57], C. Hadjivasiliou[5], G. Haefeli[41], C. Haen[40], S.C. Haines[49], B. Hamilton[60], X. Han[12], T.H. Hancock[57], S. Hansmann-Menzemer[12], N. Harnew[57], S.T. Harnew[48], C. Hasse[40], M. Hatch[40], J. He[63], M. Hecker[55], K. Heinicke[10], A. Heister[9], K. Hennessy[54], L. Henry[71], E. van Herwijnen[40], M. Heß[67], A. Hicheur[2], D. Hill[57], P.H. Hopchev[41], W. Hu[65], W. Huang[63], Z.C. Huard[59], W. Hulsbergen[43], T. Humair[55], M. Hushchyn[35], D. Hutchcroft[54], P. Ibis[10], M. Idzik[28], P. Ilten[47], R. Jacobsson[40], J. Jalocha[57], E. Jans[43], A. Jawahery[60], F. Jiang[3], M. John[57], D. Johnson[40], C.R. Jones[49], C. Joram[40], B. Jost[40], N. Jurik[57], S. Kandybei[45], M. Karacson[40], J.M. Kariuki[48], S. Karodia[53], N. Kazeev[35], M. Kecke[12], F. Keizer[49], M. Kelsey[61], M. Kenzie[49], T. Ketel[44], E. Khairullin[35], B. Khanji[12], C. Khurewathanakul[41], K.E. Kim[61], T. Kirn[9], S. Klaver[19], K. Klimaszewski[29], T. Klimkovich[11], S. Koliiev[46], M. Kolpin[12], R. Kopecna[12], P. Koppenburg[43], S. Kotriakhova[31], M. Kozeiha[5], L. Kravchuk[34], M. Kreps[50], F. Kress[55], P. Krokovny[36,w], W. Krupa[28], W. Krzemien[29], W. Kucewicz[27,l], M. Kucharczyk[27], V. Kudryavtsev[36,w], A.K. Kuonen[41], T. Kvaratskheliya[32,40], D. Lacarrere[40], G. Lafferty[56], A. Lai[16], G. Lanfranchi[19], C. Langenbruch[9], T. Latham[50], C. Lazzeroni[47], R. Le Gac[6], A. Leflat[33,40], J. Lefrançois[7], R. Lefèvre[5], F. Lemaitre[40], E. Lemos Cid[39], P. Lenisa[17], O. Leroy[6], T. Lesiak[27], B. Leverington[12], P.-R. Li[63], T. Li[3], Y. Li[7], Z. Li[61], X. Liang[61], T. Likhomanenko[68], R. Lindner[40], F. Lionetto[42], V. Lisovskyi[7], X. Liu[3], D. Loh[50], A. Loi[16], I. Longstaff[53], J.H. Lopes[2], D. Lucchesi[23,o], M. Lucio Martinez[39], A. Lupato[23], E. Luppi[17,g], O. Lupton[40], A. Lusiani[24], X. Lyu[63], F. Machefert[7], F. Maciuc[30], V. Macko[41], P. Mackowiak[10], S. Maddrell-Mander[48], O. Maev[31,40], K. Maguire[56], D. Maisuzenko[31], M.W. Majewski[28], S. Malde[57], B. Malecki[27], A. Malinin[68], T. Maltsev[36,w], G. Manca[16,f], G. Mancinelli[6], D. Marangotto[22,q], J. Maratas[5,v], J.F. Marchand[4], U. Marconi[15], C. Marin Benito[38], M. Marinangeli[41], P. Marino[41], J. Marks[12], G. Martellotti[26], M. Martin[6], M. Martinelli[41], D. Martinez Santos[39], F. Martinez Vidal[71], A. Massafferri[1], R. Matev[40], A. Mathad[50], Z. Mathe[40], C. Matteuzzi[21], A. Mauri[42], E. Maurice[7,b], B. Maurin[41], A. Mazurov[47], M. McCann[55,40], A. McNab[56], R. McNulty[13], J.V. Mead[54], B. Meadows[59], C. Meaux[6], F. Meier[10], N. Meinert[67], D. Melnychuk[29], M. Merk[43], A. Merli[22,q], E. Michielin[23], D.A. Milanes[66], E. Millard[50], M.-N. Minard[4], L. Minzoni[17], D.S. Mitzel[12], A. Mogini[8], J. Molina Rodriguez[1,y], T. Mombächer[10], I.A. Monroy[66], S. Monteil[5], M. Morandin[23], G. Morello[19], M.J. Morello[24,t], O. Morgunova[68], J. Moron[28], A.B. Morris[52], R. Mountain[61], F. Muheim[52], M. Mulder[43], D. Müller[40], J. Müller[10], K. Müller[42], V. Müller[10], P. Naik[48], T. Nakada[41], R. Nandakumar[51], A. Nandi[57], I. Nasteva[2], M. Needham[52], N. Neri[22], S. Neubert[12], N. Neufeld[40], M. Neuner[12], T.D. Nguyen[41], C. Nguyen-Mau[41,n], S. Nieswand[9], R. Niet[10], N. Nikitin[33], A. Nogay[68], D.P. O'Hanlon[15], A. Oblakowska-Mucha[28], V. Obraztsov[37], S. Ogilvy[19], R. Oldeman[16,f], C.J.G. Onderwater[72], A. Ossowska[27], J.M. Otalora Goicochea[2], P. Owen[42], A. Oyanguren[71], P.R. Pais[41], A. Palano[14], M. Palutan[19,40], G. Panshin[70], A. Papanestis[51], M. Pappagallo[52], L.L. Pappalardo[17,g], W. Parker[60], C. Parkes[56], G. Passaleva[18,40], A. Pastore[14], M. Patel[55], C. Patrignani[15,e], A. Pearce[40], A. Pellegrino[43], G. Penso[26], M. Pepe Altarelli[40], S. Perazzini[40], D. Pereima[32], P. Perret[5], L. Pescatore[41], K. Petridis[48], A. Petrolini[20,h], A. Petrov[68], M. Petruzzo[22,q], B. Pietrzyk[4], G. Pietrzyk[41], M. Pikies[27], D. Pinci[26], F. Pisani[40], A. Pistone[20,h], A. Piucci[12], V. Placinta[30], S. Playfer[52], M. Plo Casasus[39], F. Polci[8], M. Poli Lener[19], A. Poluektov[50], N. Polukhina[69], I. Polyakov[61], E. Polycarpo[2], G.J. Pomery[48], S. Ponce[40], A. Popov[37], D. Popov[11,40], S. Poslavskii[37], C. Potterat[2], E. Price[48], J. Prisciandaro[39], C. Prouve[48], V. Pugatch[46], A. Puig Navarro[42], H. Pullen[57], G. Punzi[24,p], W. Qian[63], J. Qin[63], R. Quagliani[8], B. Quintana[5], B. Rachwal[28], J.H. Rademacker[48], M. Rama[24], M. Ramos Pernas[39], M.S. Rangel[2], I. Raniuk[45,†], F. Ratnikov[35,x], G. Raven[44], M. Ravonel Salzgeber[40], M. Reboud[4],

JHEP06(2018)100

F. Redi[41], S. Reichert[10], A.C. dos Reis[1], C. Remon Alepuz[71], V. Renaudin[7], S. Ricciardi[51], S. Richards[48], K. Rinnert[54], P. Robbe[7], A. Robert[8], A.B. Rodrigues[41], E. Rodrigues[59], J.A. Rodriguez Lopez[66], A. Rogozhnikov[35], S. Roiser[40], A. Rollings[57], V. Romanovskiy[37], A. Romero Vidal[39,40], M. Rotondo[19], M.S. Rudolph[61], T. Ruf[40], J. Ruiz Vidal[71], J.J. Saborido Silva[39], N. Sagidova[31], B. Saitta[16,f], V. Salustino Guimaraes[62], C. Sanchez Mayordomo[71], B. Sanmartin Sedes[39], R. Santacesaria[26], C. Santamarina Rios[39], M. Santimaria[19], E. Santovetti[25,j], G. Sarpis[56], A. Sarti[19,k], C. Satriano[26,s], A. Satta[25], D.M. Saunders[48], D. Savrina[32,33], S. Schael[9], M. Schellenberg[10], M. Schiller[53], H. Schindler[40], M. Schmelling[11], T. Schmelzer[10], B. Schmidt[40], O. Schneider[41], A. Schopper[40], H.F. Schreiner[59], M. Schubiger[41], M.H. Schune[7,40], R. Schwemmer[40], B. Sciascia[19], A. Sciubba[26,k], A. Semennikov[32], E.S. Sepulveda[8], A. Sergi[47], N. Serra[42], J. Serrano[6], L. Sestini[23], P. Seyfert[40], M. Shapkin[37], Y. Shcheglov[31,†], T. Shears[54], L. Shekhtman[36,w], V. Shevchenko[68], B.G. Siddi[17], R. Silva Coutinho[42], L. Silva de Oliveira[2], G. Simi[23,o], S. Simone[14,d], N. Skidmore[12], T. Skwarnicki[61], I.T. Smith[52], M. Smith[55], l. Soares Lavra[1], M.D. Sokoloff[59], F.J.P. Soler[53], B. Souza De Paula[2], B. Spaan[10], P. Spradlin[53], F. Stagni[40], M. Stahl[12], S. Stahl[40], P. Stefko[41], S. Stefkova[55], O. Steinkamp[42], S. Stemmle[12], O. Stenyakin[37], M. Stepanova[31], H. Stevens[10], S. Stone[61], B. Storaci[42], S. Stracka[24,p], M.E. Stramaglia[41], M. Straticiuc[30], U. Straumann[42], S. Strokov[70], J. Sun[3], L. Sun[64], K. Swientek[28], V. Syropoulos[44], T. Szumlak[28], M. Szymanski[63], S. T'Jampens[4], A. Tayduganov[6], T. Tekampe[10], G. Tellarini[17], F. Teubert[40], E. Thomas[40], J. van Tilburg[43], M.J. Tilley[55], V. Tisserand[5], M. Tobin[41], S. Tolk[40], L. Tomassetti[17,g], D. Tonelli[24], R. Tourinho Jadallah Aoude[1], E. Tournefier[4], M. Traill[53], M.T. Tran[41], M. Tresch[42], A. Trisovic[49], A. Tsaregorodtsev[6], A. Tully[49], N. Tuning[43,40], A. Ukleja[29], A. Usachov[7], A. Ustyuzhanin[35], U. Uwer[12], C. Vacca[16,f], A. Vagner[70], V. Vagnoni[15], A. Valassi[40], S. Valat[40], G. Valenti[15], R. Vazquez Gomez[40], P. Vazquez Regueiro[39], S. Vecchi[17], M. van Veghel[43], J.J. Velthuis[48], M. Veltri[18,r], G. Veneziano[57], A. Venkateswaran[61], T.A. Verlage[9], M. Vernet[5], M. Vesterinen[57], J.V. Viana Barbosa[40], D. Vieira[63], M. Vieites Diaz[39], H. Viemann[67], X. Vilasis-Cardona[38,m], A. Vitkovskiy[43], M. Vitti[49], V. Volkov[33], A. Vollhardt[42], B. Voneki[40], A. Vorobyev[31], V. Vorobyev[36,w], C. Voß[9], J.A. de Vries[43], C. Vázquez Sierra[43], R. Waldi[67], J. Walsh[24], J. Wang[61], Y. Wang[65], D.R. Ward[49], H.M. Wark[54], N.K. Watson[47], D. Websdale[55], A. Weiden[42], C. Weisser[58], M. Whitehead[9], J. Wicht[50], G. Wilkinson[57], M. Wilkinson[61], M.R.J. Williams[56], M. Williams[58], T. Williams[47], F.F. Wilson[51,40], J. Wimberley[60], M. Winn[7], J. Wishahi[10], W. Wislicki[29], M. Witek[27], G. Wormser[7], S.A. Wotton[49], K. Wyllie[40], Y. Xie[65], M. Xu[65], Q. Xu[63], Z. Xu[3], Z. Xu[4], Z. Yang[3], Z. Yang[60], Y. Yao[61], H. Yin[65], J. Yu[65], X. Yuan[61], O. Yushchenko[37], K.A. Zarebski[47], M. Zavertyaev[11,c], L. Zhang[3], Y. Zhang[7], A. Zhelezov[12], Y. Zheng[63], X. Zhu[3], V. Zhukov[9,33], J.B. Zonneveld[52], S. Zucchelli[15]

[1] *Centro Brasileiro de Pesquisas Físicas (CBPF), Rio de Janeiro, Brazil*
[2] *Universidade Federal do Rio de Janeiro (UFRJ), Rio de Janeiro, Brazil*
[3] *Center for High Energy Physics, Tsinghua University, Beijing, China*
[4] *Univ. Grenoble Alpes, Univ. Savoie Mont Blanc, CNRS, IN2P3-LAPP, Annecy, France*
[5] *Clermont Université, Université Blaise Pascal, CNRS/IN2P3, LPC, Clermont-Ferrand, France*
[6] *Aix Marseille Univ, CNRS/IN2P3, CPPM, Marseille, France*
[7] *LAL, Univ. Paris-Sud, CNRS/IN2P3, Université Paris-Saclay, Orsay, France*
[8] *LPNHE, Université Pierre et Marie Curie, Université Paris Diderot, CNRS/IN2P3, Paris, France*
[9] *I. Physikalisches Institut, RWTH Aachen University, Aachen, Germany*
[10] *Fakultät Physik, Technische Universität Dortmund, Dortmund, Germany*
[11] *Max-Planck-Institut für Kernphysik (MPIK), Heidelberg, Germany*
[12] *Physikalisches Institut, Ruprecht-Karls-Universität Heidelberg, Heidelberg, Germany*
[13] *School of Physics, University College Dublin, Dublin, Ireland*

JHEP06(2018)100

[14] *Sezione INFN di Bari, Bari, Italy*
[15] *Sezione INFN di Bologna, Bologna, Italy*
[16] *Sezione INFN di Cagliari, Cagliari, Italy*
[17] *Universita e INFN, Ferrara, Ferrara, Italy*
[18] *Sezione INFN di Firenze, Firenze, Italy*
[19] *Laboratori Nazionali dell'INFN di Frascati, Frascati, Italy*
[20] *Sezione INFN di Genova, Genova, Italy*
[21] *Sezione INFN di Milano Bicocca, Milano, Italy*
[22] *Sezione di Milano, Milano, Italy*
[23] *Sezione INFN di Padova, Padova, Italy*
[24] *Sezione INFN di Pisa, Pisa, Italy*
[25] *Sezione INFN di Roma Tor Vergata, Roma, Italy*
[26] *Sezione INFN di Roma La Sapienza, Roma, Italy*
[27] *Henryk Niewodniczanski Institute of Nuclear Physics Polish Academy of Sciences, Kraków, Poland*
[28] *AGH - University of Science and Technology, Faculty of Physics and Applied Computer Science, Kraków, Poland*
[29] *National Center for Nuclear Research (NCBJ), Warsaw, Poland*
[30] *Horia Hulubei National Institute of Physics and Nuclear Engineering, Bucharest-Magurele, Romania*
[31] *Petersburg Nuclear Physics Institute (PNPI), Gatchina, Russia*
[32] *Institute of Theoretical and Experimental Physics (ITEP), Moscow, Russia*
[33] *Institute of Nuclear Physics, Moscow State University (SINP MSU), Moscow, Russia*
[34] *Institute for Nuclear Research of the Russian Academy of Sciences (INR RAS), Moscow, Russia*
[35] *Yandex School of Data Analysis, Moscow, Russia*
[36] *Budker Institute of Nuclear Physics (SB RAS), Novosibirsk, Russia*
[37] *Institute for High Energy Physics (IHEP), Protvino, Russia*
[38] *ICCUB, Universitat de Barcelona, Barcelona, Spain*
[39] *Instituto Galego de Física de Altas Enerxías (IGFAE), Universidade de Santiago de Compostela, Santiago de Compostela, Spain*
[40] *European Organization for Nuclear Research (CERN), Geneva, Switzerland*
[41] *Institute of Physics, Ecole Polytechnique Fédérale de Lausanne (EPFL), Lausanne, Switzerland*
[42] *Physik-Institut, Universität Zürich, Zürich, Switzerland*
[43] *Nikhef National Institute for Subatomic Physics, Amsterdam, The Netherlands*
[44] *Nikhef National Institute for Subatomic Physics and VU University Amsterdam, Amsterdam, The Netherlands*
[45] *NSC Kharkiv Institute of Physics and Technology (NSC KIPT), Kharkiv, Ukraine*
[46] *Institute for Nuclear Research of the National Academy of Sciences (KINR), Kyiv, Ukraine*
[47] *University of Birmingham, Birmingham, United Kingdom*
[48] *H.H. Wills Physics Laboratory, University of Bristol, Bristol, United Kingdom*
[49] *Cavendish Laboratory, University of Cambridge, Cambridge, United Kingdom*
[50] *Department of Physics, University of Warwick, Coventry, United Kingdom*
[51] *STFC Rutherford Appleton Laboratory, Didcot, United Kingdom*
[52] *School of Physics and Astronomy, University of Edinburgh, Edinburgh, United Kingdom*
[53] *School of Physics and Astronomy, University of Glasgow, Glasgow, United Kingdom*
[54] *Oliver Lodge Laboratory, University of Liverpool, Liverpool, United Kingdom*
[55] *Imperial College London, London, United Kingdom*
[56] *School of Physics and Astronomy, University of Manchester, Manchester, United Kingdom*
[57] *Department of Physics, University of Oxford, Oxford, United Kingdom*
[58] *Massachusetts Institute of Technology, Cambridge, MA, United States*
[59] *University of Cincinnati, Cincinnati, OH, United States*
[60] *University of Maryland, College Park, MD, United States*
[61] *Syracuse University, Syracuse, NY, United States*

JHEP06(2018)100

[62] Pontifícia Universidade Católica do Rio de Janeiro (PUC-Rio), Rio de Janeiro, Brazil, associated to[2]
[63] University of Chinese Academy of Sciences, Beijing, China, associated to[3]
[64] School of Physics and Technology, Wuhan University, Wuhan, China, associated to[3]
[65] Institute of Particle Physics, Central China Normal University, Wuhan, Hubei, China, associated to[3]
[66] Departamento de Fisica , Universidad Nacional de Colombia, Bogota, Colombia, associated to[8]
[67] Institut für Physik, Universität Rostock, Rostock, Germany, associated to[12]
[68] National Research Centre Kurchatov Institute, Moscow, Russia, associated to[32]
[69] National University of Science and Technology MISIS, Moscow, Russia, associated to[32]
[70] National Research Tomsk Polytechnic University, Tomsk, Russia, associated to[32]
[71] Instituto de Fisica Corpuscular, Centro Mixto Universidad de Valencia - CSIC, Valencia, Spain, associated to[38]
[72] Van Swinderen Institute, University of Groningen, Groningen, The Netherlands, associated to[43]
[73] Los Alamos National Laboratory (LANL), Los Alamos, United States, associated to[61]

[a] Universidade Federal do Triângulo Mineiro (UFTM), Uberaba-MG, Brazil
[b] Laboratoire Leprince-Ringuet, Palaiseau, France
[c] P.N. Lebedev Physical Institute, Russian Academy of Science (LPI RAS), Moscow, Russia
[d] Università di Bari, Bari, Italy
[e] Università di Bologna, Bologna, Italy
[f] Università di Cagliari, Cagliari, Italy
[g] Università di Ferrara, Ferrara, Italy
[h] Università di Genova, Genova, Italy
[i] Università di Milano Bicocca, Milano, Italy
[j] Università di Roma Tor Vergata, Roma, Italy
[k] Università di Roma La Sapienza, Roma, Italy
[l] AGH - University of Science and Technology, Faculty of Computer Science, Electronics and Telecommunications, Kraków, Poland
[m] LIFAELS, La Salle, Universitat Ramon Llull, Barcelona, Spain
[n] Hanoi University of Science, Hanoi, Vietnam
[o] Università di Padova, Padova, Italy
[p] Università di Pisa, Pisa, Italy
[q] Università degli Studi di Milano, Milano, Italy
[r] Università di Urbino, Urbino, Italy
[s] Università della Basilicata, Potenza, Italy
[t] Scuola Normale Superiore, Pisa, Italy
[u] Università di Modena e Reggio Emilia, Modena, Italy
[v] Iligan Institute of Technology (IIT), Iligan, Philippines
[w] Novosibirsk State University, Novosibirsk, Russia
[x] National Research University Higher School of Economics, Moscow, Russia
[y] Escuela Agrícola Panamericana, San Antonio de Oriente, Honduras
[†] Deceased

JHEP06(2018)100